Carbohydrate Polymers 105 (2014) 308–316

Contents lists available at ScienceDirect

Carbohydrate Polymers

journal homepage: www.elsevier.com/locate/carbpol

Chain conformation and anti-tumor activity of derivatives of polysaccharide from *Rhizoma Panacis Japonici*

Cong Chen [a], Wenhua Wu [a], Xiaojuan Xu [a,*], Lina Zhang [a,*], Ying Liu [b], Kaiping Wang [b]

[a] Department of Chemistry, Wuhan University, Wuhan 430072, China
[b] Tongji Medical College, Huazhong University of Science and Technology, Wuhan 430030, China

ARTICLE INFO

Article history:
Received 17 October 2013
Received in revised form 13 January 2014
Accepted 27 January 2014
Available online 4 February 2014

Keywords:
Carboxymethylated polysaccharide
Sulfated polysaccharide
Phosphated polysaccharide
Chain conformation
Anti-tumor activity

ABSTRACT

A hyper branched (1→4)-α-D-glucan (RPS3) with degree of branching of 35% extracted from *Rhizoma Panacis Japonici* adopted a sphere-like conformation and showed little bioactivity. Three derivatives including sulfated (S-), phosphated (P-) and carboxymethylated (CM-) RPS3 were then synthesized and characterized by FTIR, ^{13}CNMR, and SEC-LLS-Vis-RI. As a result, the molecular weights of CM-RPS3, S-RPS3 and P-RPS3 decreased sharply in contrast to the original one, suggesting that chemical degradation has occurred. Moreover, the sphere-like conformation of RPS3 transferred into the random coil-like conformation according to the increased values of α_η, α_s and ρ. It was ascribed to the occurrence of the preferential degradation for the branches. *In vitro* and *in vivo* tests demonstrated that the negatively charged S-RPS3 and P-RPS3 with properly low molecular mass significantly inhibited H-22 tumor cells growth. This work offered valuable results for broadening the biological applications of α-D-glucans.

1. Introduction

Traditional Chinese herbal medicines have been demonstrated with various bioactivities, such as antibacterial (Hamasaki et al., 2000), antiviral (Kobayashi, Davis, Utsunomiya, Pollard, & Suzuki, 1999), antitumor (Liao et al., 2005; Tang et al., 2003a,b), antipyretic (Ni, Zhang, Hou, Shi, & Guo, 2009), diuretic (Wright, Van-Buren, Kroner, & Koning, 2007), anti-inflammatory (Xu, Yasuda, Nakamura-Tsuruta, Mizuno, & Ashida, 2012) and antihypertensive (Liu et al., 2003) activities. In particular, the bioactivities of individual component of the Chinese herbal medicines have been followed with great interest (Cao & Lin, 2002; Huang, Jin, Zhang, Cheung, & Kennedy, 2007; Wang et al., 2011). *Rhizoma Panacis Japonici*, a Chinese traditional medicine, is usually treated as a substitute for Panax Ginseng, whose root is now widely used in treating many diseases (Huang & Zhang, 2009). The apozem has been always considered to have anti-inflammatory and anti-aging activities, but the therapeutic mechanism of its extract has not been established at full length. Recently, the structures and chain conformations of five kinds of water-soluble polysaccharides coded as RPS1, RPS2, RPS3, RPS4 and RPS5 extracted stepwise from *Rhizoma Panacis Japonici* by using 0.9% NaCl aqueous solution at 25 °C, boiling water at 120 °C, 0.5 M NaOH/0.01 M $NaBH_4$ at 10 °C, 1.0 M NaOH/0.02 M $NaBH_4$ at 10 °C and 19 M HCOOH at 4 °C, respectively, have been already investigated in our lab. All the five polysaccharides were highly branched (1→4)-α-D-glucan heteropolysaccharides, and the values of degree of branch (*DB*) were in the range of 35–45%. (Huang & Zhang, 2009; Huang, Huang, Li, & Zhang, 2009; Huang, Ren, Duan, & Zhang, 2010). Of these, RPS3 has far more yield (3.62%) than others, and showed better water-solubility. However, it showed little bioactivity.

Normally, the polysaccharides with anti-tumor activities have (1→3)-β-glucan as the backbone. Moreover, the anti-tumor activities are dependent on the molecular weight and water-solubility of polysaccharides. It has been reported that the polysaccharides with good water-solubility and suitable molecular weight may exhibit higher antitumor activities (Leung, Liu, Koon, & Fung, 2006; Misaki, Kakuta, Sasaki, Tanaka, & Miyaji, 1981; Wasser, 2002). It is noteworthy that polysaccharide derivates would have a large variety of functions and biological activities. In recent years, many studies have been focused on the structures and biological properties of polysaccharide derivatives, especially the sulfated, phosphated and carboxymethylated derivatives (Huang & Zhang, 2011; Wijesinghe & Jeon, 2012; Zhang, Cheung, Zhang, Chiu, & Ooi, 2004). Sulfated polysaccharides with potential health benefits and numerous biological activities including anticoagulant, antithrombotic, anticancer and their inflammatory and immune responses have been

* Corresponding authors. Tel.: +86 27 87219274/27 68754188; fax: +86 27 68762005/27 68754188.
E-mail addresses: xuxj@whu.edu.cn (X. Xu), zhangln@whu.edu.cn (L. Zhang).

0144-8617/$ – see front matter © 2014 Elsevier Ltd. All rights reserved.
http://dx.doi.org/10.1016/j.carbpol.2014.01.089

studied extensively (Wijesinghe & Jeon, 2012; Campo, Kawano, da Silva, & Carvalho, 2009; Wijesekara, Pangestuti, & Kim, 2011). The phosphated polysaccharides exhibit anti-inflammatory, anti-cancer and anti-viral activities, and the introduction of phosphate group can conspicuously improve the biological activities. However, the substituting degree of the phosphated polysaccharides reported in literatures has been very low so that they were not widely investigated in general (Huang & Zhang, 2011; Lyuksutova et al., 2005). Carboxymethyl substitution has been considered to be another efficacious method to improve the functional properties, such as antioxidant and immunomodulatory activities (Shin, Lee, Bae, Yoo, & Lee, 2007; Wang, Zhang, Yu, & Cheung, 2009; Yang et al., 2011; Zhang et al., 2004). Moreover, the primary usage of this derivatization was to increase water solubility of chitin and cellulose and obtain functionalized materials from them (Fan et al., 2013; Karabulut, Pettersson, Ankerfors, & Wågberg, 2012).

Most of the researchers focused on the polysaccharides with a backbone of β-glucan, and the bioactivities of polysaccharides derivatives with a backbone of (1→4)-α-D-glucan have been scarcely reported. Based on the above, the objective of this work was to get an individual component of the polysaccharides from *Rhizoma Panacis Japonici*, and prepare three kinds of derivatives of water-soluble polysaccharide RPS3 for ultilization of traditional Chinese herbal medicine of *Rhizoma Panacis Japonic*. To investigate their molecular weights, structures and chain conformations, size-exclusion chromatography combined with laser light scattering, differential refractive index detector and viscometer (SEC-MALLS-Vis-RI combination) was used. The *in vitro* and *in vivo* antitumor activities of the samples were also measured to give a broad insight of the factors which would influence bioactivities. This work would give an insight that α-glucans after derivatization also possessed bioactivity, which will broad the biological applications of α-D-glucans.

2. Experimental

2.1. Materials

Rhizoma Panacis Japonici (RPJ) was cultivated in Enshi, Hubei Province, China. The dried RPJ was smashed into pieces, and defatted sequentially by Soxhlet extractor with ethyl acetate and acetone for 6 h respectively. The resultant residue was immersed in 0.9% NaCl aqueous stirring for 24 h at room temperature and centrifuged at 6000 rpm for 30 min to obtain the residues. Subsequently, the residues were immersed in distilled water at 120 °C for half an hour. After centrifugation, the residues were extracted with 0.5 M NaOH/0.01 M $NaBH_4$ at 10 °C for 4 h, and the mixture was centrifuged and neutralized with acetic acid. The resultant supernate was concentrated by rotary evaporator, followed by deproteining *via* Savage method and discoloring with H_2O_2. The supernate was dialyzed using regenerated cellulose tubes (M_w cut-off 8000, USA) against distilled water for five days and ultrapure water for three days, and then lyophilized. Afterwards white powder-like polysaccharide coded as RPS3 was obtained with the productivity of 3.62%. GC–MS total ion current (TIC) chromatogram of methylation analyses was performed as described in our previous work (Huang & Zhang, 2009). GC–MS was carried out on a GCT system (Macro-Mass, Waters, USA) with a capillary GC column (HP-5MS, 30 m × 0.32 mm ID × 0.25 m, Agilent, USA), helium (He) was used as carrier gas.

2.2. Carboxymethylation

Carboxymethyl RPS3 was prepared as follows. According to the procedure reported by Bao, Duan, Fang, and Fang (2001), parent polysaccharide (500 mg) was suspended in 15 mL of 2-propanol at room temperature. Afterwards 10 mL of 30% NaOH aqueous was slowly added within 15 min, and then 3 g of chloroacetic acid was added. The mixture was heated to 50 °C for 2 h and the resultant was neutralized with HCl. The solution was dialyzed with regenerated cellulose tubes (M_w cut-off 8000, USA) against distilled water for seven days. White scale-like carboxymethylated derivative (CM-RPS3) was obtained after lyophilizing, and the yield was 93.5%.

2.3. Sulfation

RPS3 was sulfated according to the method of Yoshida et al. (1995). Briefly, 500 mg of RPS3 was dissolved in 20 mL of dimethylsulfoxide with stirring at room temperature overnight to get a limpid solution. Subsequently, 3 mL of pyridine was added into the solution, and then chlorosulfonic acid (1.24 mL) was added drop wise with constantly stirring in an ice bath. The system was allowed to react for 2 h at 60 °C. The reacted product was neutralized with 5% NaOH aqueous. Finally the resultant solution was dialyzed with regenerated cellulose tubes (M_w cut-off 8000, USA) against distilled water for seven days to remove pyridine and inorganic molecules, and then lyophilized to get the light-yellow sample coded as S-RPS3 with the yield of 98.1%.

2.4. Phosphorylation

Williams's method was employed to prepare the phosphorylated derivative (Williams et al., 1991). In brief, 400 mg of RPS3 was dissolved in 20 mL of dimethylsulfoxide along with 7.2 g urea. Then 3 mL of H_3PO_4 was slowly added into the reacted mixture. The mixture was allowed to react at 100 °C for 6 h. Subsequently, the reacted product was dialyzed with regenerated cellulose tubes (M_w cut-off 8000, USA) against distilled water for seven days, and then lyophilized to obtain white powder derivative coded as P-RPS3 with the yield of 61.2%.

2.5. Structural characterization

Infrared (IR) spectra of RPS3 and its derivatives were recorded on a Nicolet 5700 Fourier transform infrared spectroscopy (FTIR) (Spectrum One, Perkin Elmer Co., Madison, WI) in the range of 4000–400 cm^{-1} using the KBr-disk method. ^{13}C NMR spectroscopy measurements of the samples were analyzed on a Mercury 300 NMR spectrometer (Varian Inc., Palo Alto, CA, USA) at room temperature. 99.96% D_2O was used as the solvent. The elemental compositions of C, H, N and S in RPS3 and its derivatives were determined by elemental analyzer (Vario Micro cube, Elementar Co., Germany). The percentage of P element in P-RPS3 was detected by inductively coupled plasma atomic emission spectrometer (IRIS Intrepid II XSP, Thermo Electron Co., USA). The degree of substitution (*DS*) of CM-RPS3 was calculated according to the method of conductance titration (Muzzarelli et al., 1984). Accurate 0.1 g of samples was dissolved in 0.1 M HCl (50 mL) and the solution was titrated with 0.1 M NaOH. To determine the number of carboxymethyl groups in the sample, the value of conductivity was measured with a conductivity meter. The percentage of C element in the substituent group was calculated with the equation as follows:

$$C\% = 24 \times (V_2 - V_1) \times \frac{C_{NaOH}}{m} \quad (1)$$

where V_1 and V_2 represent the volume of NaOH during the platform, C_{NaOH} is the concentration of NaOH and m is the mass of the sample.

2.6. Characterization of molecular weight and chain conformation

The molecular weight and chain conformational parameters of RPS3 and its derivatives were detected with SEC-MALLS-Vis-RI combination technology. Specifically, the weight-average molecular weight (M_w) and radius of gyration ($\langle S^2\rangle_z^{1/2}$) of RPS3 and its derivatives were determined by a size exclusion chromatography (Column Shodex OHPAK SB-805 HQ, 8.0 mm × 300 mm) combined with multi-angle laser light scattering system (SEC-LLS) and a Waters 515 HPLC Pump. A He–Ne laser (λ = 663.4 nm) was equipped (Dawn Heleos-II, Wyatt Technology Co., USA) with different angles ranging from 13° to 158°. The basic light-scattering equation is as follows (Zimm, 1948):

$$\frac{Kc}{R_\theta} = \frac{1}{M_W}\left[1 + \frac{16\pi^2 n^2 \langle S^2\rangle_z}{3\lambda^2}\mathrm{Sin}^2\left(\frac{\theta}{2}\right)\right] + 2A_2 c + \cdots \quad (2)$$

where K represents the optical constant which equals to $[4\pi^2 n^2 (\mathrm{d}n/\mathrm{d}c)^2]/(\lambda^4 N_A)$, c, the polymer concentration in the unit of mg/mL; R_θ, the Rayleigh ratio; λ, the wavelength in vacuum; n, the refractive index of the solvent at λ; dn/dc, the refractive index increment; N_A, the Avogadro number, and A_2, the second viral coefficient. The values of specific refractive index increment (dn/dc) of RPS3, CM-RPS3, S-RPS3 and P-RPS3 in 0.9% NaCl aqueous were determined to be 0.145, 0.141, 0.121 and 0.148 mL/g, separately. The eluent was selected to be 0.9% NaCl aqueous at a flow rate of 0.50 mL/min, which was degassed with a degasser (Flom Gastorr TG-14, USA), and the column was kept at 40 °C by a CBL model 200 column heater. A viscometer (Viscostar-II viscometer, Wyatt Technology Co., USA) was simultaneously connected to give the value of the intrinsic viscosities ([η]). Huggins and Kraemer equations were used to estimate the value of [η] (Huggins, 1942).

$$\frac{\eta_{sp}}{c} = [\eta] + k'[\eta]^2 c \quad (3)$$

$$\frac{\ln \eta_r}{c} = [\eta] - \left(\frac{1}{2} - k'\right)[\eta]^2 c \quad (4)$$

Here, k' is a constant for a given polymer under the desired conditions, η_{sp}/c, the reduced viscosity, and $\ln \eta_r/c$, the inherent viscosity. Besides, a differential refractive index detector (Optilab T-rEX, Wyatt Technology Co., USA) was combined to detect the polysaccharide concentration, and a software of Astra (Version 6.1.1.17) was used to collect and analysis the data. All the samples were optically purified by a filter of 0.2 μm (PTFE, Puradisc 13-mm Syringe Filters, Whatman, England). The values of specific refractive index increment (dn/dc) of RPS3 and its derivatives in 0.9% NaCl aqueous were measured with an Optilab refractometer (DAWN DSP, Wyatt Technology Co., USA). In details, the samples with a series of gradient concentrations were obtained and injected into the optilab detector with a manual injection valve. The data was collected and processed *via* the Wyatt Technology's Windows-based DNDCTM software.

2.7. In vitro anti-tumor activities against mouse hepatoma H-22 cells

Mouse hepatoma H-22 cell line (kindly provided by Tongji Medical College of the Huazhong University of Science and Technology) was employed to the assays of the *in vitro* and *in vivo* anti-tumor activities. The H-22 cell line was cultivated in mouse's ascites and extracted with syringe. Cells were incubated in the culture medium of Roswell Park Memorial Institute (RPMI) 1640 medium supplemented with 10% fetal bovine serum (FBS), 100 μg/mL streptomycin and 100 U/mL penicillin. A colorimetric 3-(4, 5-dimethylthiazol-2-yl)-2, 5-diphenyltetrazolium bromide (MTT) method was used to measure the proliferation of cells (Mosmann, 1983).

The culture medium above was used to prepare suspensions of H-22 cells with the concentration of 1×10^5 cells/mL, 100 μL of the suspensions were seeded in wells of a 96-well microplate. 100 μL of different sample solutions (with the concentrations from 400 μg/mL to 6.25 μg/mL) and Tris-Pt (12.5 μg/mL) which was used as the positive control were added into the wells separately. The culture medium was added in wells as the negative control group. Then the 96-well microplate was incubated at 37 °C in a humidified atmosphere of 5% carbon dioxide for 24 h. Afterwards, cells in each well were incubated in 50 μL of MTT (5 mg/mL) for another 4 h at the same condition. The microplate was centrifuged to remove the supernatant, and 100 μL of DMSO was added into each well. A microplate ELISA reader (Bio-Tek EL × 800, USA) was used to detect the optical density (OD) value of the solutions in each cell at 570 nm. All *in vitro* results were expressed as the inhibition ratio (Φ) of H-22 cell proliferation as follows:

$$\Phi = \frac{OD_a - OD_b}{OD_a} \times 100\% \quad (5)$$

where OD_a and OD_b are the absorbance values of negative control group and sample groups, respectively.

2.8. In vivo antitumor assay

Sterile clean BALB/c male mice with body weight of 20–21 g were provided by Animal Biosafety Level-III Laboratory from Wuhan University. H-22 cells extracted from tumor-bearing mice were subcutaneously implanted into the right-hand groin of each mouse at a dose of about 1×10^5 cells/mouse. After 24 h, different concentration (5 mg/kg, 40 mg/kg) of samples dissolved in 0.9% NaCl aqueous were injected intraperitoneally once daily for 10 days, and cyclophosphamide (30 mg/kg) was used as a positive control. The same volume of 0.9% NaCl aqueous was injected into the negative control mice. After 10 days, the mice were executed, and the tumors were weighed. The antitumor activities were expressed as the inhibition ratio (ξ) as follows:

$$\xi = \frac{W_c - W_t}{W_c} \times 100\% \quad (6)$$

where W_c and W_t are the average tumor weights of control group and tested groups. The spleen index and thymus index were calculated as follows:

$$I_s = \frac{W_s}{W_m} \times 10 \quad (7)$$

$$I_t = \frac{W_t}{W_m} \times 10 \quad (8)$$

where W_s and W_t represent the weights of the spleen and thymus of the mice respectively, and W_m is the weights of the mice.

To investigate the tumor morphology, the tumor tissues were cut slightly at a size of 3–5 mm and thickness of 3 mm and fixed in 4% paraformaldehyde. Afterwards, the tumors were dehydrated by immersing in a series from 60%, 70%, 80%, 90%, and 95% to 100% of gradient ethanol solution for 15–40 min. Dehydrated-tumors were treated with methyl benzoate until all ethanol was replaced by methyl benzoate. Subsequently, the tumors were embedded in the paraffin. Finally, 4 mm serial sections were cut from the paraffin-embedded pretreatment tumor blocks and mounted on poly-L-lysine (PLL)-coated microscope slides, followed by drying at 62°C for 4 h and then immunostaining. After sealed with neutral gum and cover slip, the tumor tissues were observed by optical microscope.

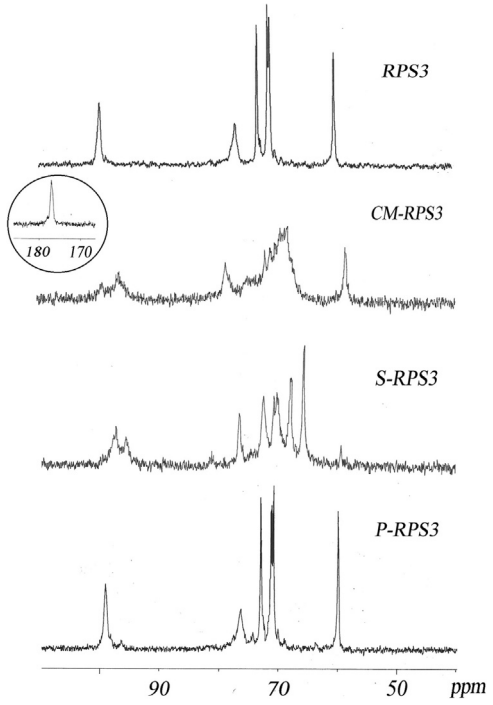

Fig. 1. ^{13}C NMR spectra for native sample RPS3 and its derivatives CM-RPS3, S-RPS3 and P-RPS3 in D_2O at 25 °C.

2.9. Statistical analysis

Statistical analysis was performed with Student's *t*-test to evaluate the differences between the control and sample groups, and the *P* values less than 0.05 were considered to be statically significant.

3. Results and discussion

3.1. Chemical structure

The structure of RPS3 has been detected in our previous work, and it was proved to have glucose and galactose residues, which was identified as a (1→4)-α-D-glucan with one branched residue for every six main chain glucose residues (Huang & Zhang, 2009). The FTIR spectra of RPS3 and its derivatives are shown in Supporting Information Figure S1. For RPS3, the peaks at 1240 cm^{-1}, 1420 cm^{-1} and 1650 cm^{-1} exhibited the characteristic absorption of polysaccharide. In addition, the obvious characteristic absorption peaks at 930 cm^{-1} and 850 cm^{-1} were assigned to α-D-glucan (Barker, Bourne, Stacey, & Whiffen, 1954; Cui et al., 2008; Wu & Tu, 2005). The spectra of CM-RPS3, S-RPS3 and P-RPS3 indicated that the substitution has occurred successfully (detailed structure analysis in supporting information). For the native polysaccharide RPS3, the degree of branching (*DB*) could be calculated with the result from GC/MS *via* the following equation:

$$DB = \frac{N_T + N_B}{N_T + N_B + N_L} \tag{9}$$

where, N_T, N_B and N_L are the numbers of the terminal residues, branch residues and linear residues, respectively (Tao, Zhang, Yan, & Wu, 2007). The value of *DB* was calculated to be 35%, indicating that RPS3 was a kind of hyper branched polysaccharide.

The ^{13}C NMR spectra of RPS3 and the derivatives are shown in Fig. 1, and the chemical shifts are listed in Supporting Information Table S1. The spectra of RPS3 exhibited six major signals at around 99.9, 77.2, 73.6, 71.8, 71.4 and 60.6 ppm, assigned to C-1, C-4, C-3, C-5, C-2 and C-6, respectively, further conforming that the RPS3 sample was a (1→4)-α-D-glucan. Clearly, the signals of galactose residues at 106.6, 73.8, 75.8, 71.1, 78.5 and 64.1 ppm (Liu, Dong, Dong, Fang, and Ding, 2007) were very weak, indicating that RPS3 was mainly composed of glucose. In comparison to the spectrum of RPS3, there were several new signals in that of CM-RPS3. The peaks at 75.4, 78.9 and 67.3 ppm were assigned to the signal of C-2s, C-3s and C-6s, separately. In addition, the peak at 97.3 ppm was attributed to the signal of C-1′, and the upfield splitting was caused by the influence of the partial substitution of the adjacent C-2 and C-6 (Gorin, 1981; Zhang, Wang, & Zhang, 2010). Notably, the peak at 70.3 ppm was assigned to the methylene of $-CH_2COO^-$ (C-7). Clearly, the peak for carboxyl carbon was at 176.8 ppm (C-8), indicating the substitution of carboxymethyl groups had occurred. In the spectra of S-RPS3, the C-1 was also split into two peaks, one was at around 97.8 ppm and the other was at 95.9 ppm. The regular peaks for C-2, C-3, C-4, C-5 and C-6 were at 71.0, 73.0, 77.2, 71.2 and 59.9 ppm, respectively, corresponding to that of RPS3 sample. And the substituent carbons showed chemical shifts at 76.7, 81.7 and 66.4 ppm, assigned to C-2s, C-3s and C-6s. It is notable that the signal at 66.4 ppm for C-6s was stronger than others, and the native C-6 exhibited a weak peak, which could be explained by the assumption that the most substitution occurred at C-6 position (Huang & Zhang, 2005). Regrettably, the spectra of P-RPS3 exhibited no clear information for the phosphorylated groups because of the low degree of substitution. Very weak peaks at 74.3, 77.3 and 63.6 ppm might represent C-2s, C-3s and C-6s respectively, indicating the similar degree of substitution at the three carbon positions.

The degree of substitution (*DS*) values for S-RPS3 and P-RPS3 were designed as the average number of substituent group on each sugar residue. The values can be calculated from the elemental composition in the polysaccharides (*S*% and *P*%) on the basis of Schöniger's formula (Schöniger, 1956):

$$DS_S = \frac{162 \times S\%}{32 - 102 \times S\%} \tag{10}$$

$$DS_P = \frac{162 \times P\%}{31 - 97 \times P\%} \tag{11}$$

As for CM-RPS3, *C*% represents the percentage of C element only in the substituent groups (Muzzarelli et al., 1984). The degree of substitution can also be calculated by the following empirical formula:

$$DS_{CM} = \frac{162 \times C\%}{24 - 58 \times C\%} \tag{12}$$

The *DS* values for CM-RPS3, S-RPS3 and P-RPS3 were thus calculated to be 0.93, 0.91 and 0.18, indicating the substitution really occurred. All the samples were water-soluble, and the water solubility of the derivatives improved after derivatization. The yields, water solubility, and values of *DS* are summarized in Supporting Information Table S2. According to the results above, the derivatization was considered to be random substitution both on C-2s, C-3s and C-6s. Furthermore, because of the hyper branched structure of RPS3, the side chains surrounding had access to the derivatization reagent easily, and thus the functional groups were primarily inserted in the side chains.

3.2. Molecular weight and chain configuration

Since 0.9% NaCl aqueous has been extensively used in multifarious bioactivity assays, it was adopted in this section. When the samples were dissolved in water, the derivatives would exhibit electrostatic repulsion effect because of the charged groups. The electrostatic repulsion effect could be eliminated by adding salt (Wang & Zhang, 2009). Additionally, the intrinsic viscosity of RPS3

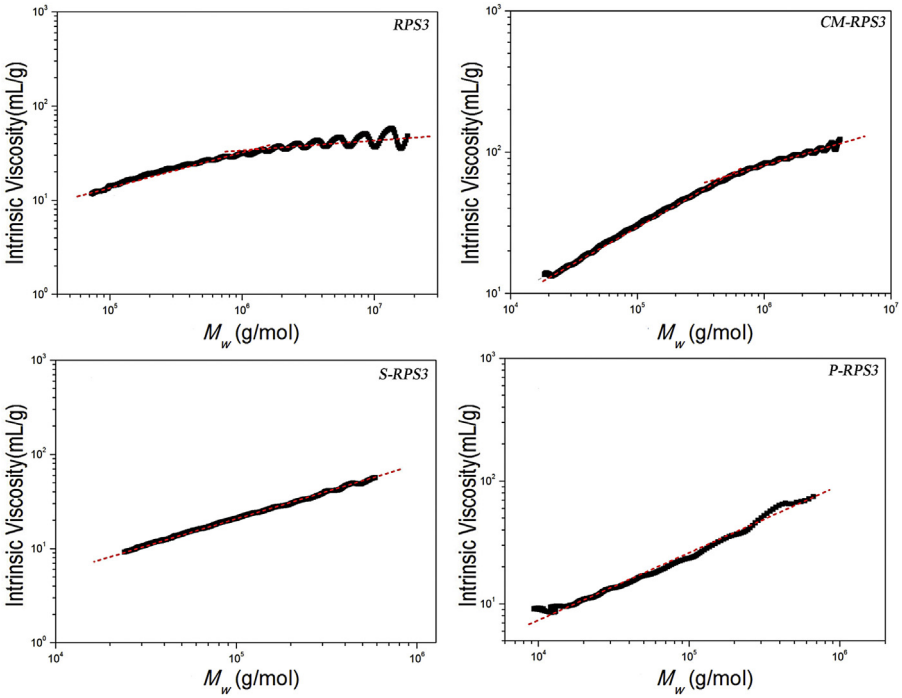

Fig. 2. Dependence of intrinsic viscosity $[\eta]$ on M_w for RPS3 and its derivatives in 0.9% NaCl aqueous solution at 25 °C.

in 0.9% NaCl aqueous was measured by using a Ubbelohde type, and the Huggins' constant k' was estimated to be 0.32, suggesting that 0.9% NaCl aqueous was a good solvent for RPS3. Thus, 0.9% NaCl aqueous was used to determinate the molecular mass and chain configuration of RPS3 and its derivatives.

In our laboratory, SEC-MALLS-Vis-RI combination instrument has been used to detect the weight-average molecular weight (M_w), root mean square radius of gyration ($\langle S^2\rangle_z^{1/2}$), intrinsic viscosity ($[\eta]$) and hydrodynamic radius (R_h) of polysaccharides synchronously. Supporting Information Figure S2 shows the light scattering signals of the samples in 0.9% NaCl. Clearly, the peak position moved to the point with longer retention time after derivatization in the order of RPS3, CM-RPS3, S-RPS3 and P-RPS3. In general, the retention time depends on the molecular size, and the polymers with larger molecular size flew out preferentially while those with smaller molecular size exhibited long retention time. The scattering intensity was also decreased after derivatization in the same order, suggesting that the molecular weight of RPS3 decreased after derivatization. The calculated results of M_w, R_h, $\langle S^2\rangle_z^{1/2}$ and $[\eta]$ of the samples in 0.9% NaCl aqueous solution are listed in Table 1. It can be seen that the M_w of RPS3 sharply decreased after derivatization. In particular, the M_w of S-RPS3 and P-RPS3 were much lower than that of the RPS3, demonstrating that chemical degradation occurred during the process of derivatization.

By using SEC-MALLS-Vis-RI combination instrument, the values of M_w, $\langle S^2\rangle_z^{1/2}$ and $[\eta]$ were detected as numerous experimental points, thus the relationships of $M_W - \langle S^2\rangle_z^{1/2}$ and $M_w - [\eta]$ can be obtained. Figs. 2 and 3 show the double logarithmic relationship of the $M_w - [\eta]$ (Mark–Houwink equation plots) and $M_W - \langle S^2\rangle_z^{1/2}$ of the four samples in 0.9% NaCl aqueous solution. The exponent α_η of $M_w - [\eta]$ and α_s of $M_W - \langle S^2\rangle_z^{1/2}$ are well known to be related to the shape of the macromolecules and the nature of the solvent. Usually, the value of α_η is 0.5–0.8 for flexible chain conformation and 1–2 for a semi-flexible or stiff chain (Shukla et al., 1991; Xu, Xu, & Zhang, 2012), and the values of α_s are 0.33, 0.50–0.60 and 1 for globular shape, flexible chain conformation and rigid rod chain, separately (Chen, Xu, Zhang, & Zeng, 2009). The values of α_η and α_s lower than 0.5 indicates the polymer is hyper branched. As shown in Table 1, the low values of α_η (0.35) and α_s (0.30) of RPS3 conformed its hyper branched structure discussed in the structural analysis, and suggested RPS3 adopted a sphere-like conformation. After derivatization, the values of α_η and α_s increased. Very interesting, the sulfated and phosphorylated derivatives exhibited relatively high values of α_η and α_s, which lie in the range of linear random coils.

Macromolecular parameter $\rho(\rho \equiv \langle S^2\rangle_z^{1/2}/R_h)$ was another criterion for chain conformation of the polymers. The radius of gyration ($\langle S^2\rangle_z^{1/2}$) is regarded as the mean square of the distance between the segment and the mass center, whereas the hydrodynamic radius (R_h) is defined as the parameter to characterize the dimension of macromolecules in solution taking into account the hydrodynamic interactions. Normally, when ρ approximates to be 0.77, the polymer adopts the hard sphere conformation; $\rho = 1.0$–1.1 corresponds to the highly branched chain, and 1.5–1.8 for flexible chain configuration; $\rho > 2$ indicating the worm-like or stiff chain (Niu, Liaw, Sang, & Wu, 2000). The ρ values of the original and derivatized samples are summarized in Table 1. The value for RPS3 was 1.18, also indicating that the native polysaccharide has hyper branched structure. The ρ values of the derivatives were almost in the range of 1.5–1.8, which were in good agreement with the results from α_η, α_s and $[\eta]$.

Taken together, all the three conformational parameters of α_η, α_s and ρ demonstrated that RPS3 was highly branched and adopted a sphere-like conformation, while a coil-like conformation after derivatization. As discussed above, the chains of RPS3 were chemically cleaved during derivatization. Were the main chain or the branches broken? As shown in Table 2, the M_w of RPS3 was much higher than those of CM-RPS3, S-RPS, and P-RPS3, but the $[\eta]$ value was lower than CM-RPS3 and S-RPS3, suggesting that the *DB* of CM-RPS3 and S-RPS3 decreased in contrast to RPS3. Namely, the chemical cleavage preferentially occurred in the branches, leading to an increase in α_η, α_s and ρ.

Table 1
Experiment results from SEC-MALLS-Vis-RI for RPS3 and its derivatives in 0.9% NaCl aqueous at 25 °C.

Samples	dn/dc	$M_w \times 10^{-4}$	M_w/M_n	$\langle S^2\rangle_Z^{1/2}$ (nm)	R_h (nm)	$[\eta]$ (cm^3 g^{-1})	α_s	α_η	ρ ($\equiv\langle S^2\rangle_z^{1/2}/R_h$)
RPS3	0.145	76.5	3.00	44.7	37.9	19.4	0.30	0.35	1.18
CM-RPS3	0.141	33.0	1.69	19.6	10.8	39.1	0.41	0.43	1.81
S-RPS3	0.121	12.1	1.67	17.5	9.8	22.1	0.55	0.58	1.79
P-RPS3	0.148	4.1	1.87	9.2	6.1	14.1	0.51	0.52	1.51

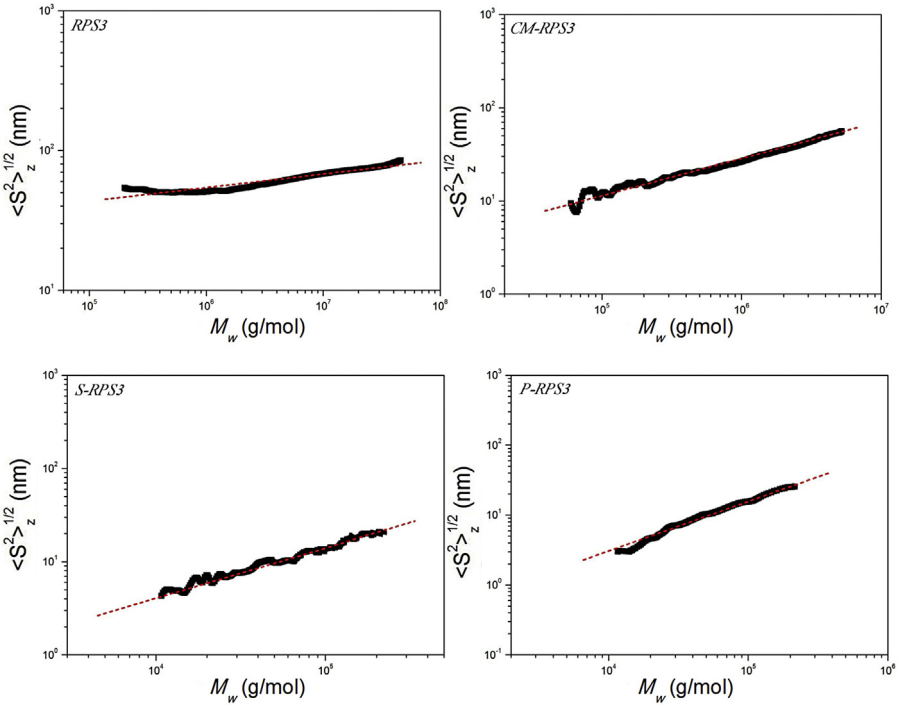

Fig. 3. Dependence of $\langle S^2\rangle_Z^{1/2}$ on M_w for RPS3 and its derivatives in 0.9% NaCl aqueous solution at 25 °C.

Table 2
Results of *in vivo* antitumor activities and the spleen index and thymus index of the samples compared with cyclophosphamide.

Samples	Dose (mg/kg × days)	Inhibition ratio (ξ %)	Spleen index (I_s mg/g)	Thymus index (I_t mg/g)	Survival/test mice
0.9% NaCl	–	–	4.01	1.11	7/8
RPS3	5	11.2	4.66	1.38	8/8
	40	16.8	4.73	1.02	7/8
CM-RPS3	5	22.3	4.77	1.12	8/8
	40	29.2	4.54	0.91	8/8
S-RPS3	5	32.1	4.68	0.92	8/8
	40	34.4	4.32	1.10	8/8
P-RPS3	5	25.8	4.33	0.84	8/8
	40	52.4	4.67	0.72	8/8
CTX	30	40.4	2.83	0.43	7/8

To clarify the position of chemical degradation, a linear polysaccharide PCS3-II from *Poria cocos* was choosed as the reference after derivatization by the same methods as RPS3 derivatives, and characterized by using SEC-MALLS-Vis-RI (see Supporting Information Figure S3). The $[\eta]$ data of the RPS3 derivatives were lower than those of PCS3-II derivatives in the same range of molecular weight, suggesting that the RPS3 derivatives were still branched. The relatively high values of α_η, α_s and ρ revealed that the branches were short, leading them to looking like a linear random coil.

3.3. Antitumor activities against mouse hepatoma H-22 cells in vitro

The derivatives exhibited inhibition against Mouse Hepatoma H-22 cells proliferation *in vitro* at different concentrations, and the

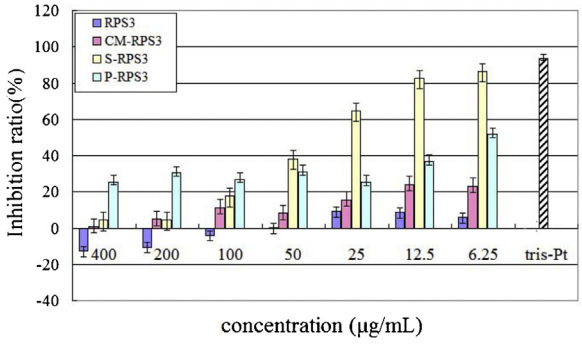

Fig. 4. Percentage of viability of H-22 cells treated with native RPS3 and its derivatives at different concentrations. Data are shown as mean standard deviation (SD) ($n = 3$).

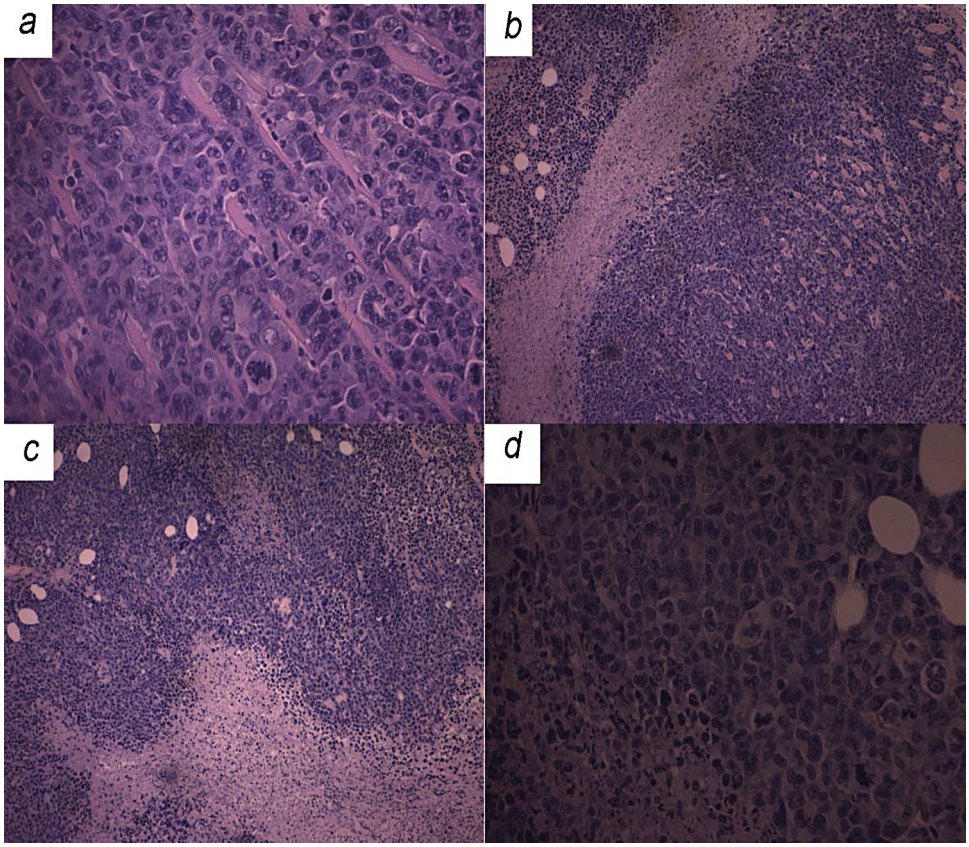

Fig. 5. Pictures of stained mouse tumor tissues under optical microscope: (a) negative control group × 400, (b) dose 40 mg/kg S-RPS3 treated mice group × 100, (c) dose 40 mg/kg P-RPS3 treated mice group × 100, (d) dose 40 mg/kg P-RPS3 treated mice group × 400.

results are shown in Fig. 4. Tris-Pt, a well known antitumor agent, was also involved for comparison. Apparently, the original polysaccharide RPS3 was proved to have no specific bioactivities at any concentration. CM-RPS3 presented little antitumor activity at relatively low concentration. However, certain inhibition ratios caused by S-RPS3 and P-RPS3 against H-22 cells were observed after 24 h incubation. Especially for S-RPS3, an unambiguous dose-dependent relationship was clearly observed, and S-RPS3 samples exhibited strong antitumor activity comparable with Tris-Pt at relatively low concentrations (25, 12.5, 6.25 μg/mL). The charged polysaccharide at relatively high concentration may entangle with each other, so that the effective groups may be shielded. Interestingly, the inhibition ratio of P-RPS3 showed no tendency of decreasing with increasing the concentration. The phenomenon may account for the fact that during the process of phosphorylation, the polysaccharide crushed into pieces because of the high temperature, and the *DS* value was relatively low. Thus in the solution of P-RPS3 with experimental concentrations, the charged groups were separated clearly and effective to inhibit H-22 cells. Furthermore, S-RPS3 and P-RPS3 possessed relatively low molecular weights but inhibited *in vitro* proliferation of S-180 tumor cells more effectually, confirming that the proper low molecular weight was important to anti-tumor activity. In view of these results, the molecular weight, chain conformation and charged groups could act as vital factors in bioactivities.

3.4. Antitumor activities against H-22 solid tumor in BALB/c male mice

Antitumor activities *in vivo* were further investigated to reveal the mechanism of actions. Intra-peritoneal injection of the four samples above at different doses was adopted once daily for 10 days after H-22 tumor cells inoculation for 24 h. The surviving numbers and inhibition of tumor growth are summarized in Table 2. RPS3 displayed little antitumor activity not only *in vitro* but also *in vivo*. However, the inhibition ratios of S-RPS3 and R-RPS3 reached 34.4% and 52.4% at the dose of 40 mg/kg respectively. These values were close to that of cyclophosphamide (CTX), a widely used antitumor drug in living organism. Interestingly, the weight enhancement of the experimental groups was notably higher than that of positive control group. In addition, the spleen index and thymus index suggested that, unlike cyclophosphamide which gave rise to great damage to the immune organs, all the polysaccharide samples were low toxicity. So S-RPS3 and P-RPS3 can be used as potential antitumor agents.

Fig. 5 shows the internal morphology of the tumor tissues by the optical microscope in different groups. In the negative control group (Fig. 5a), the tumor cells grew normally and arranged in irregular nests structures, the blood vessels could be observed like the hepatic sinusoid. The tumor cells came in wide variety sizes and morphology, exhibiting obvious mitotic figures and atypia. The tumor tissues of the mice under the treatment with S-RPS3 and P-RPS3 (Fig. 5b and c) showed massive necrosis induced with nucleus atrophy and chromatin condensation. From the figures many membrane-enclosed apoptotic bodies can be observed, indicating the undergoing apoptosis. Fig. 5d was clearer to observe the morphology of tumor cells under the treatment with P-RPS3 at dose of 40 mg/kg. At the lower left corner was the necrosis area of tumor cells, and cell microstructure digested and tissues without determined structure appeared. In general, the samples of S-RPS3 and P-RPS3 inhibited the growth of H-22 tumor cells *in vivo* remarkably under the process of cell apoptosis.

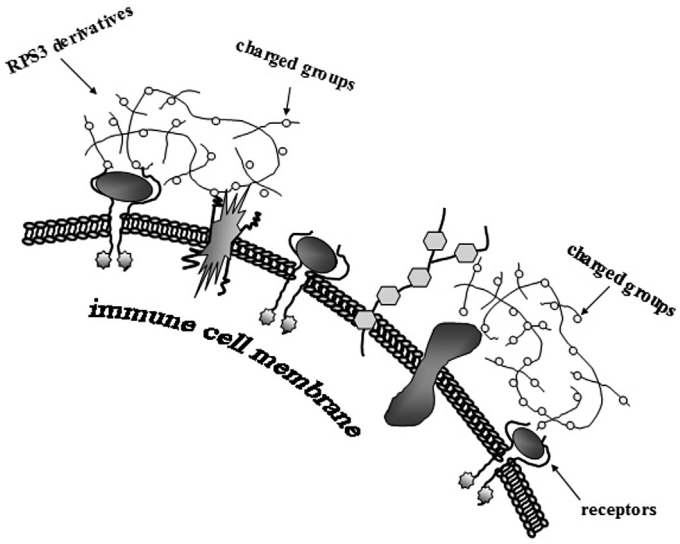

Fig. 6. The schematic diagram for the interaction between the chains of RPS3 derivatives and receptors from immune cell membrane.

In addition, the anti-tumor activities induced by polysaccharides were considered to be associated with the activation of immune system, and the macrophages were significant immune cells. By activating the macrophages, helper T cells were activated, thus the immune response occurred (Moradali, Mostafavi, Ghods, & Hedjaroude, 2007; Schepetkin & Quinn, 2006). It has been reported that the polysaccharides significantly activated the macrophages (Lee et al., 2006; Chen et al., 2008). Besides the substitute groups, molecular weights and chain configurations also played important roles in anti-tumor activities of S-RPS3 and P-RPS3. RPS3 derivatives with higher α value adopted relatively expanded chain conformations, and the expanded chains provided more exposed groups. Overall, thanks to their relatively more extended chains, negative charges and proper molecular weights, S-RPS3 and P-RPS3 enjoyed more opportunities to act with the receptors of the macrophages, leading to the effective immune response. The schematic diagram of mechanism is shown in Fig. 6.

4. Conclusion

A water-soluble hyper branched (1→4)-α-D-glucan (RPS3) with degree of branching (*DB*) value of 35% was successfully used to synthesize the carboxymethyl polysaccharides (CM-RPS3), the sulfated polysaccharides (S-RPS3) and the phosphated polysaccharides (P-RPS3) in 2-propanol or DMSO solutions. SEC-MALLS-Vis-RI combination instrument was used to characterize their molar weights and chain conformations successfully. The results illustrated that RPS3 adopted condensed coil conformation, and the derivatives adopted more extended flexible coil conformation, indicating the chain extensibility depended on the type of substituent groups and degree of substitution. Anti-tumor activity assays indicated that, S-RPS3 and P-RPS3 exhibited prominent inhibition against H-22 tumor cells whatever *in vitro* and *in vivo*; S-RPS3 showed higher activity *in vitro* while P-RPS3 *in vivo*. Therefore, the polysaccharides with negative charges and proper molecular weights possessed higher anti-tumor activity. That might result from the truth that the factors above endow polysaccharides more opportunities to bind with receptors on the surface of cells. This work would give an insight that α-glucans after derivatization also possessed bioactivity, which will broad their biological applications of α-D-glucans.

Acknowledgements

This work was supported by National Basic Research Program of China (973 Program, 2010CB732203), the major grants of the National Natural Science Foundation of China (21334005 and 30530850), and National Natural Science Foundation of China (21274114).

Appendix A. Supplementary data

Supplementary data associated with this article can be found, in the online version, at http://dx.doi.org/10.1016/j.carbpol.2014.01.089.

References

Bao, X., Duan, J., Fang, X., & Fang, J. (2001). Chemical modifications of the (1→3)-α-D-glucan from spores of *Ganoderma lucidum* and investigation of their physicochemical properties and immunological activity. *Carbohydrate Research*, *336*, 127–140.

Barker, S. A., Bourne, E. J., Stacey, M., & Whiffen, D. H. (1954). Infra-red spectra of carbohydrates. Part I. Some derivatives of D-glucopyranose. *Journal of the American Chemical Society*, 171–176.

Campo, V. L., Kawano, D. F., da Silva, D. B., Jr., & Carvalho, I. (2009). Carrageenans: Biological properties, chemical modifications and structural analysis – A review. *Carbohydrate Polymers*, *77*, 167–180.

Cao, L., & Lin, Z. (2002). Regulation on maturation and function of dendritic cells by *Ganoderma lucidum* polysaccharides. *Immunology Letters*, *83*, 163–169.

Chen, X., Lu, J., Zhang, Y., He, J., Guo, X., Tian, G., et al. (2008). Studies of macrophage immuno-modulating activity of polysaccharides isolated from *Paecilomyces tenuipes*. *International Journal of Biological Macromolecules*, *43*, 252–256.

Chen, X., Xu, X., Zhang, L., & Zeng, F. (2009). Chain conformation and anti-tumor activities of phosphorylated (1→3)-β-D-glucan from *Poria cocos*. *Carbohydrate Polymers*, *78*, 581–587.

Cui, H., Liu, Q., Tao, Y., Zhang, H., Zhang, L., & Ding, K. (2008). Structure and chain conformation of a (1→6)-α-D-glucan from the root of *Pueraria lobata* (Willd.) Ohwi and the antioxidant activity of its sulfated derivative. *Carbohydrate Polymers*, *74*, 771–778.

Fan, L., Tan, C., Wang, L., Pan, X., Cao, M., Wen, F., et al. (2013). Preparation, characterization and the effect of carboxymethylated chitosan–cellulose derivatives hydrogels on wound healing. *Journal of Applied Polymer Science*, *128*, 2789–2796.

Gorin, P. A. J. (1981). Carbon-13 nuclear magnetic resonance spectroscopy of polysaccharides. *Advances in Carbohydrate Chemistry and Biochemistry*, *38*, 13–104.

Hamasaki, N., Ishii, E., Tominaga, K., Tezuka, Y., Nagaoka, T., Kadota, S., et al. (2000). Highly selective antibacterial activity of novel alkyl quinolone alkaloids from a Chinese herbal medicine, Gosyuyu (Wu-Chu-Yu), against *Helicobacter pylori* in vitro. *Microbiology and Immunology*, *44*, 9–15.

Huang, Q., Jin, Y., Zhang, L., Cheung, P. C. K., & Kennedy, J. F. (2007). Structure, molecular size and antitumor activities of polysaccharides from *Poria cocos* mycelia produced in fermenter. *Carbohydrate Polymers*, *70*, 324–333.

Huang, Q., & Zhang, L. (2011). Preparation, chain conformation and anti-tumor activities of water-soluble phosphated (1→3)-α-D-glucan from *Poria cocos* mycelia. *Carbohydrate Polymers*, *83*, 1363–1369.

Huang, Q., & Zhang, L. (2005). Solution properties of (1→3)-α-D-glucan and its sulfated derivative from *Poria cocos* mycelia via fermentation tank. *Biopolymers*, *79*, 28–38.

Huang, Z., Huang, Y., Li, X., & Zhang, L. (2009). Molecular mass and chain conformations of *Rhizoma Panacis Japonici* polysaccharides. *Carbohydrate Polymers*, *78*, 596–601.

Huang, Z., Ren, H., Duan, X., & Zhang, L. (2010). Chain conformation and bioactivity of water-soluble polysaccharide extracted from *Rhizoma Panacis Japonici*. *Biopolymers*, *93*, 383–390.

Huang, Z., & Zhang, L. (2009). Chemical structures of water-soluble polysaccharides from *Rhizoma Panacis Japonici*. *Carbohydrate Research*, *344*, 1136–1140.

Huggins, M. L. (1942). The viscosity of dilute solutions of long-chain molecules. IV. Dependence on concentration. *Journal of the American Chemical Society*, *64*, 2716–2718.

Karabulut, E., Pettersson, T., Ankerfors, M., & Wågberg, L. (2012). Adhesive layer-by-layer films of carboxymethylated cellulose nanofibril-dopamine covalent bioconjugates inspired by marine mussel threads. *ACS Nano*, *6*, 4731–4739.

Kobayashi, M., Davis, S. M., Utsunomiya, T., Pollard, R. B., & Suzuki, F. (1999). Antiviral effect of Gingyo-San, a traditional Chinese herbal medicine, on influenza A2 virus infection in mice. *American Journal of Chinese Medicine*, *27*, 53–62.

Lee, K. Y., Lee, M. H., Chang, I. Y., Yoon, S. P., Lim, D. Y., & Jeon, Y. J. (2006). Macrophage activation by polysaccharide fraction isolated from *Salicornia herbacea*. *Journal of Ethnopharmacology*, *103*, 372–378.

Leung, M. Y. K., Liu, C., Koon, J. C. M., & Fung, K. P. (2006). Polysaccharide biological response modifiers. *Immunology Letters*, *105*, 101–114.

Liao, C. H., Pan, S. L., Guh, J. H., Chang, Y. L., Pail, H. C., Lin, C. H., et al. (2005). Antitumor mechanism of evodiamine, a constituent from Chinese herb *Evodiae fructus*, in

human multiple-drug resistant breast cancer NCI/ADR-RES cells in vitro and in vivo. *Carcinogenesis*, *26*, 968–975.
Liu, L., Dong, Q., Dong, X., Fang, J., & Ding, K. (2007). Structural investigation of two neutral polysaccharides isolated from rhizome of Polygonatum sibiricum. *Carbohydrate Polymers*, *70*, 304–309.
Liu, J. C., Hsu, F. L., Tsai, J. C., Chan, P., Liu, J. Y. H., Thomas, G. N., et al. (2003). Antihypertensive effects of tannins isolated from traditional Chinese herbs as non-specific inhibitors of angiotensin converting enzyme. *Life Sciences*, *73*, 1543–1555.
Lyuksutova, O. I., Murphey, E. D., Toliver-Kinsky, T. E., Lin, C. Y., Cui, W. H., Williams, D. L., et al. (2005). Glucan phosphate treatment attenuates burn-induced inflammation and improves resistance to *Pseudomonas aeruginosa* burn wound infection. *Shock*, *23*, 224–232.
Misaki, A., Kakuta, M., Sasaki, T., Tanaka, M., & Miyaji, H. (1981). Studies on interrelation of structure and antitumor effects of polysaccharides: Antitumor action of periodate-modified, branched (1→3)-beta-D-glucan of *Auricularia auricula-judae*, and other polysaccharides containing (1→3)-glycosidic linkages. *Carbohydrate Research*, *92*, 115–129.
Moradali, M. F., Mostafavi, H., Ghods, S., & Hedjaroude, G. A. (2007). Immunomodulating and anticancer agents in the realm of macromycetes fungi (macrofungi). *International Immunopharmacology*, *7*, 701–724.
Mosmann, T. (1983). Rapid colorimetric assay for cellular growth and survival: Application to proliferation and cytotoxicity assays. *Journal of Immunological Methods*, *65*, 55–63.
Muzzarelli, R. A. A., Tanfani, F., Emanuelli, M., Pace, D. P., Chiurazzi, E., & Piani, M. (1984). Sulfated N-(carboxymethyl) chitosans: Novel blood anticoagulants. *Carbohydrate Research*, *126*, 225–231.
Ni, L., Zhang, L., Hou, J., Shi, W., & Guo, M. (2009). A strategy for evaluating antipyretic efficacy of Chinese herbal medicines based on UV spectra fingerprints. *Journal of Ethnopharmacology*, *124*, 79–86.
Niu, A., Liaw, D. J., Sang, H. C., & Wu, C. (2000). Light-scattering study of a zwitterionic polycarboxybetaine in aqueous solution. *Macromolecules*, *33*, 3492–3494.
Schepetkin, I. A., & Quinn, M. T. (2006). Botanical polysaccharides: macrophage immunomodulation and therapeutic potential. *International Immunopharmacology*, *6*, 317–333.
Schöniger, W. (1956). Rapid microanalytical determinations of halogens and sulfur in organic substances. *Microchemistry Acta*, *4*, 869–876.
Shin, J. Y., Lee, S. Y., Bae, I. Y., Yoo, S. H., & Lee, H. G. (2007). Structural and biological study of carboxymethylated *Phellinus linteus* polysaccharides. *Journal of Agricultural and Food Chemistry*, *55*, 3368–3372.
Shukla, P., Cotts, P. M., Miller, R. D., Russell, T. P., Smith, B. A., Wallraff, G. M., et al. (1991). Conformational transition studies of organosilane polymers by light and neutron scattering. *Macromolecules*, *24*, 5606–5613.
Tang, W., Hemm, I., & Bertram, B. (2003a). Recent development of antitumor agents from Chinese herbal medicines. Part I. Low molecular compounds. *Planta Medica*, *69*, 97–108.
Tang, W., Hemm, I., & Bertram, B. (2003b). Recent development of antitumor agents from Chinese herbal medicines. Part II. High molecular compounds. *Planta Medica*, *69*, 193–201.
Tao, Y., Zhang, L., Yan, F., & Wu, X. (2007). Chain conformation of water-insoluble hyperbranched polysaccharide from fungus. *Biomacromolecules*, *8*, 2321–2328.
Wang, J., Ma, Z., Zhang, L., Fang, Y., Jiang, F., & Philips, G. O. (2011). Structure and chain conformation of water-soluble heteropolysaccharides from *Ganoderma lucidum*. *Carbohydrate Polymers*, *86*, 844–851.
Wang, J., Zhang, L., Yu, Y., & Cheung, P. C. K. (2009). Enhancement of antitumor activities in sulfated and carboxymethylated polysaccharides of *Ganoderma lucidum*. *Journal of Agricultural and Food Chemistry*, *57*, 10565–10572.
Wang, X., & Zhang, L. (2009). Physicochemical properties and antitumor activities for sulfated derivatives of lentinan. *Carbohydrate Research*, *344*, 2209–2216.
Wasser, S. P. (2002). Medicinal mushrooms as a source of antitumor and immunomodulating polysaccharides. *Applied Microbiology and Biotechnology*, *60*, 258–274.
Wijesekara, I., Pangestuti, R., & Kim, S. K. (2011). Biological activities and potential health benefits of sulfated polysaccharides derived from marine algae. *Carbohydrate Polymers*, *84*, 14–21.
Wijesinghe, W. A. J. P., & Jeon, Y. J. (2012). Biological activities and potential industrial applications of fucose rich sulfated polysaccharides and fucoidans isolated from brown seaweeds: A review. *Carbohydrate Polymers*, *88*, 13–20.
Williams, D. L., McNamee, R. B., Jones, E. L., Pretus, H. A., Ensley, H. E., Browder, I. W., et al. (1991). A method for the solubilization of a (1→3)-β-D-glucan isolated from *Saccharomyces cerevisiae*. *Carbohydrate Research*, *219*, 203–213.
Wright, C. I., Van-Buren, L., Kroner, C. I., & Koning, M. M. G. (2007). Herbal medicines as diuretics: A review of the scientific evidence. *Journal of Ethnopharmacology*, *114*, 1–31.
Wu, X. M., & Tu, P. F. (2005). Isolation and characterization of α-(1→6)-glucans from *Cistanche deserticola*. *Journal of Asian Natural Products Research*, *7*, 823–828.
Xu, S., Xu, X., & Zhang, L. (2012). Branching structure and chain conformation of water-soluble glucan extracted from *Auricularia auricula-judae*. *Journal of Agricultural and Food Chemistry*, *60*, 3498–3506.
Xu, X., Yasuda, M., Nakamura-Tsuruta, S., Mizuno, M., & Ashida, H. (2012). β-Glucan from *Lentinus edodes* inhibits nitric oxide and tumor necrosis factor-α and phosphorylation of mitogen-activated protein kinases in lipopolysaccharide stimulated murine RAW 264.7 macrophages. *Journal of Biological Chemistry*, *287*, 871–878.
Yang, L., Zhao, T., Wei, H., Zhang, M., Zou, Y., Mao, G., et al. (2011). Carboxymethylation of polysaccharide from *Auricularia auricula* and their antioxidant activities in vitro. *International Journal of Biological Macromolecules*, *49*, 1124–1130.
Yoshida, T., Yasuda, Y., Mimura, T., Kaneko, Y., Nakashima, H., Yamamoto, N., et al. (1995). Synthesis of curdlan sulfates having inhibitory effects in vitro against AIDS viruses HIV-1 and HIV-2. *Carbohydrate Research*, *276*, 425–436.
Zhang, M., Cheung, P. C. K., Zhang, L., Chiu, C. M., & Ooi, V. E. C. (2004). Carboxymethylated β-glucans from mushroom sclerotium of *Pleurotus tuber-regium* as novel water-soluble anti-tumor agent. *Carbohydrate Polymers*, *57*, 319–325.
Zhang, Y., Wang, J., & Zhang, L. (2010). Creation of highly stable selenium nanoparticles capped with hyperbranched polysaccharide in water. *Langmuir*, *26*, 17617–17623.
Zimm, B. H. (1948). The scattering of light and the radial distribution function of high polymer solutions. *Journal of Chemical Physics*, *16*, 1093–1099.